British Journal of Cancer www.nature.com/bjc

ARTICLE

Check for updates

Cellular and Molecular Biology

SLC38A4 functions as a tumour suppressor in hepatocellular carcinoma through modulating Wnt/β-catenin/MYC/HMGCS2 axis

Jie Li[1,5], Ming-han Li[1,5], Tian-tian Wang[1,5], Xiao-ning Liu[2,5], Xiao-ting Zhu[3,5], Yun-zhang Dai[1,5], Ke-chao Zhai[1], Yong-da Liu[1], Jia-li Lin[1], Rui-liang Ge[4], Shu-han Sun[1], Fang Wang[1]✉ and Ji-hang Yuan[1]✉

BACKGROUND: Many molecular alterations are shared by embryonic liver development and hepatocellular carcinoma (HCC). Identifying the common molecular events would provide a novel prognostic biomarker and therapeutic target for HCC.
METHODS: Expression levels and clinical relevancies of SLC38A4 and HMGCS2 were investigated by qRT-PCR, western blot, TCGA and GEO datasets. The biological roles of SLC38A4 were investigated by functional assays. The downstream signalling pathway of SLC38A4 was investigated by qRT-PCR, western blot, immunofluorescence, luciferase reporter assay, TCGA and GEO datasets.
RESULTS: SLC38A4 silencing was identified as an oncofetal molecular event. DNA hypermethylation contributed to the downregulations of Slc38a4/SLC38A4 in the foetal liver and HCC. Low expression of SLC38A4 was associated with poor prognosis of HCC patients. Functional assays demonstrated that SLC38A4 depletion promoted HCC cellular proliferation, stemness and migration, and inhibited HCC cellular apoptosis in vitro, and further repressed HCC tumorigenesis in vivo. HMGCS2 was identified as a critical downstream target of SLC38A4. SLC38A4 increased HMGCS2 expression via upregulating AXIN1 and repressing Wnt/β-catenin/MYC axis. Functional rescue assays showed that HMGCS2 overexpression reversed the oncogenic roles of SLC38A4 depletion in HCC.
CONCLUSIONS: SLC38A4 downregulation was identified as a novel oncofetal event, and SLC38A4 was identified as a novel tumour suppressor in HCC.

British Journal of Cancer (2021) 125:865–876; https://doi.org/10.1038/s41416-021-01490-y

BACKGROUND

Liver cancer is the sixth most common cancer and the third leading cause of cancer-related deaths worldwide [1]. Among all malignancies, liver cancer has a relatively worse prognosis with a 5-year survival rate of <20% [2, 3]. Hepatocellular carcinoma (HCC) is the main histological subtype of liver cancer [4]. Further investigations into the critical molecular mechanisms driving HCC tumorigenesis and progression are urgently needed [5–7].

Increasing evidence have shown that HCC shares many molecular characteristics with embryonic liver development [8]. These shared molecular events could be regarded as oncofetal molecular events, such as the high expression of alpha-fetoprotein (AFP) in the foetal liver and HCC. Furthermore, those HCCs with stronger embryonic gene expression characteristics are known to have a worse prognosis [9]. Thus, further uncovering critical oncofetal events during foetal liver development and HCC would provide novel insights for HCC tumorigenesis and targets for HCC therapy. Accumulating studies have identified several common aberrant signalling pathways in HCC, such as Wnt/β-catenin, TGF-β, c-MET, RAS-MAPK, mTOR signalling and so on [10, 11]. Some of these signalling pathways were also reported to be involved in liver development, such as Wnt/β-catenin, TGF-β and c-MET signalling [12]. The molecules modulating these shared signalling pathways may be oncofetal events in HCC.

In our previous study, gene expression characteristics of mouse foetal liver and adult liver tissues were detected by microarray [13]. Combining gene expression characteristics of HCC tissues from The Cancer Genome Atlas (TCGA) Liver Hepatocellular Carcinoma (LIHC) dataset, we identified SLC38A4 downregulation as a novel oncofetal molecular event. SLC38A4 belongs to the solute carrier proteins (SLC) superfamily and is a system A amino acid transporter [14–16]. SLC38A4 is also named as neutral amino acid transporter 4 (SNAT4). Amino acids are obligatory for the survival and growth of highly proliferative cells, such as embryonic cells and cancer cells [17]. Therefore, amino acid transporters are routinely highly expressed in these proliferative cells [18]. However, SLC38A4 downregulation was identified in proliferative

[1]Department of Medical Genetics, Naval Medical University, Shanghai, China. [2]Core Facility of Basic Medical Sciences, Shanghai Jiao Tong University School of Medicine, Shanghai, China. [3]Department of Anatomy and Physiology, Shanghai Jiao Tong University School of Medicine, Shanghai, China. [4]The Second Department of Liver Surgery, Eastern Hepatobiliary Surgery Hospital, Naval Medical University, Shanghai, China. [5]These authors contributed equally: Jie Li, Ming-han Li, Tian-tian Wang, Xiao-ning Liu, Xiao-ting Zhu, Yun-zhang Dai. ✉email: wfsjz@163.com; jihangyuan@smmu.edu.cn

Received: 14 April 2021 Revised: 11 June 2021 Accepted: 8 July 2021
Published online: 17 July 2021

foetal liver and HCC cells. Therefore, we focused on this particular amino acid transporter SLC38A4.

The expression of SLC38A4 during foetal liver development and in HCC tissues were further analysed in multiple publicly available datasets and detected in our own cohort. The correlation between SLC38A4 expression and clinicopathological characteristics of HCC patients was analysed in several cohorts. Furthermore, the biological roles of SLC38A4 in HCC were investigated using cell proliferation, colony formation, spheroid formation, cell apoptosis, cell migration and in vivo tumorigenesis assays. The mechanisms of action of SLC38A4 in HCC were investigated using co-expression analysis and experimental verifications.

METHODS

Tissue samples

HCC tissues and paired noncancerous liver tissues were randomly obtained from HCC patients with written informed consent who underwent surgical resection in the Eastern Hepatobiliary Surgery Hospital affiliated to Naval Medical University (Shanghai, China). Tissue samples were collected and snap-frozen in liquid nitrogen immediately and then stored at −80 °C until use. Foetal liver samples were harvested from embryonic day 15.5 (E15.5) liver tissues. Adult liver samples were harvested from 8-week-old C57BL/6 mice. This study was performed with the approval of the Committee on Ethics of Biomedicine Research, Naval Medical University.

Cell cultures and treatments

Human HCC cells Hep3B and Huh7 were obtained from the Chinese Academy of Science Cell Bank (Shanghai, China). The cells were cultured at 37 °C in an atmosphere containing 5% CO_2 and in Eagle's Minimum Essential Medium (Hep3B) or Dulbecco's modified Eagle's medium (Huh7) supplemented with 10% foetal bovine serum (FBS). These cell lines were authenticated by short tandem repeat (STR) profiling and routinely tested as mycoplasma-free. Where indicated, cells were treated with 2.5 μM 5-Aza (cat# ab120842, Abcam, Cambridge, UK) for 3 days or 20 mM LiCl (cat# A100416, Sangon Biotech, Shanghai, China) for 24 h.

Bisulfite DNA Sequencing

DNA was extracted from indicated tissues and cells using the TIANamp Genomic DNA Kit (TIANGEN, Beijing, China) and bisulfite-treated using EZ DNA Methylation-Gold™ Kit (Zymo Research, Irvine, CA, USA). Modified genomic DNA was then PCR-amplified with the primers 5′-GTTTATGGAATTT TAGTTTAATTTTT-3′ (forward) and 5′-CCCRTAAAAAAACCCTCTTAAAAAT-3′ (reverse) for mouse CpG36; 5′-TTTTTTGTTTTTTTTTTTAGGTTT-3′ (forward) and 5′-ACACTAAATAAAAAACTTAAAATA-3′ (reverse) for human CpG64. The PCR products were gel-extracted, subcloned into pMD-19T Vectors (Takara, Dalian, China), and transformed into *Escherichia coli*. Candidate plasmid clones were sequenced by Jieli Science and technology Ltd. (Shanghai, China).

Animal studies

Male 5–6-week-old athymic BALB/c nude mice were purchased from the Shanghai Experimental Animal Center of the Chinese Academy of Sciences (Shanghai, China). The mice were maintained in a special pathogen-free class experimental animal room and kept in an environmentally controlled room (25 °C temperature, 50% humidity and light 12 h/day) with free access to fresh water and a solid pellet diet. Indicated HCC cells (2×10^6) were injected subcutaneously into the left or the right armpit of mice. Subcutaneous tumours were allowed to grow for 20 days. Then, the mice were sacrificed using excess carbon dioxide and the subcutaneous tumours were resected and weighed. For 5-Aza treatment in vivo, 5×10^6 Huh7 cells were subcutaneously inoculated into athymic BALB/c nude mice. When subcutaneous tumours were palpable, mice were randomly assigned to either the control group (vehicle) or the treatment group (intraperitoneal injection of 1 mg/kg 5-Aza every 2 days). Subcutaneous tumours were allowed to grow for another 10 days. Then, the mice were sacrificed using excess carbon dioxide, and the subcutaneous tumours were resected and weighed. No statistical method was used to determine the sample size. The experiments were not randomised. The investigators recording tumour growth were blinded to mouse allocation. The animal studies were approved by the Committee on Ethics of Biomedicine Research, Naval Medical University.

Statistical analysis

All statistical analyses were performed using the GraphPad Prism 6.0 Software. For comparisons, Student's *t* test (two-sided), one-way analysis of variance (ANOVA) followed by Dunnett's multiple comparisons test, Mann–Whitney test, Wilcoxon matched-pairs signed-rank test, Kruskal–Wallis test, log-rank test, Pearson chi-square test, and Pearson correlation analysis were performed as indicated in figure and table legends. A P value < 0.05 was considered significant.

Other methods are shown in Supplementary Information.

RESULTS

Slc38a4 is downregulated in foetal livers compared with adult livers

In our previous study of mouse foetal liver development, we detected differentially expressed genes during foetal liver development using microarray analyses (GSE57824) [13]. In this microarray result, we found that Slc38a4 was gradually increased during the mouse foetal liver development process (Fig. 1a). The same expression pattern of Slc38a4 during foetal liver development was also verified in two another publicly available datasets GSE13149 and GSE21224 (Fig. 1b, c). Furthermore, we measured Slc38a4 expression in mouse foetal liver tissues and adult liver tissues. Consistently, the results showed that Slc38a4 was downregulated in foetal liver tissues compared with adult liver tissues (Fig. 1d, e).

SLC38A4 is downregulated in HCC and negatively correlated with prognosis

We then investigated SLC38A4 expression and its clinical relevance in human HCC tissues. The Cancer Genome Atlas (TCGA) Liver Hepatocellular Carcinoma (LIHC) dataset showed that low SLC38A4 expression was remarkably correlated with poor overall survival, disease-specific survival, recurrence-free survival and progression-free survival (Supplementary Fig. 1a–d), analysed by Kaplan–Meier Plotter (https://kmplot.com/analysis/index.php). Correlation analyses between SLC38A4 expression levels and clinicopathological characteristics from TCGA LIHC dataset revealed that low SLC38A4 expression was significantly correlated with high serum AFP concentration, poor differentiation, advanced tumour pathologic pT staging, vascular invasion and advanced TNM staging (Supplementary Table 1), supporting low SLC38A4 expression as an embryonic and potential oncogenic factor. GSE14520 dataset revealed that SLC38A4 was downregulated in HCC tissues compared with noncancerous liver tissues (Fig. 2a). Kaplan–Meier survival analysis consistently revealed that low SLC38A4 expression was significantly correlated with poor overall survival according to the GSE14520 dataset (Fig. 2b). Correlation analyses between SLC38A4 expression levels and clinicopathological characteristics from the GSE14520 dataset consistently revealed that low SLC38A4 expression was significantly correlated with high serum AFP concentration, high predicted risk metastasis signature, larger main tumour size, advanced TNM staging and advanced BCLC staging (Supplementary Table 2). The downregulation of SLC38A4 in HCC was further verified in GSE54236 and GSE39791 datasets (Fig. 2c, d). GSE6764 datasets revealed that the expression of SLC38A4 was gradually downregulated during the progression of HCC (Fig. 2e). Furthermore, SLC38A4 mRNA levels in 40 pairs of randomly selected human HCC tissues and adjacent noncancerous liver tissues were measured by qRT-PCR and the results revealed that SLC38A4 mRNA levels were downregulated in HCC tissues compared with liver tissues (Fig. 2f). Western blot analyses revealed that SLC38A4 protein levels were also downregulated in HCC tissues compared with paired nontumor liver tissues (Fig. 2g). IHC staining of SLC38A4 in human tissue array including 70 pairs of HCC tissues and nontumor liver tissues revealed significantly weaker staining density of SLC38A4 in HCC tissues compared with paired

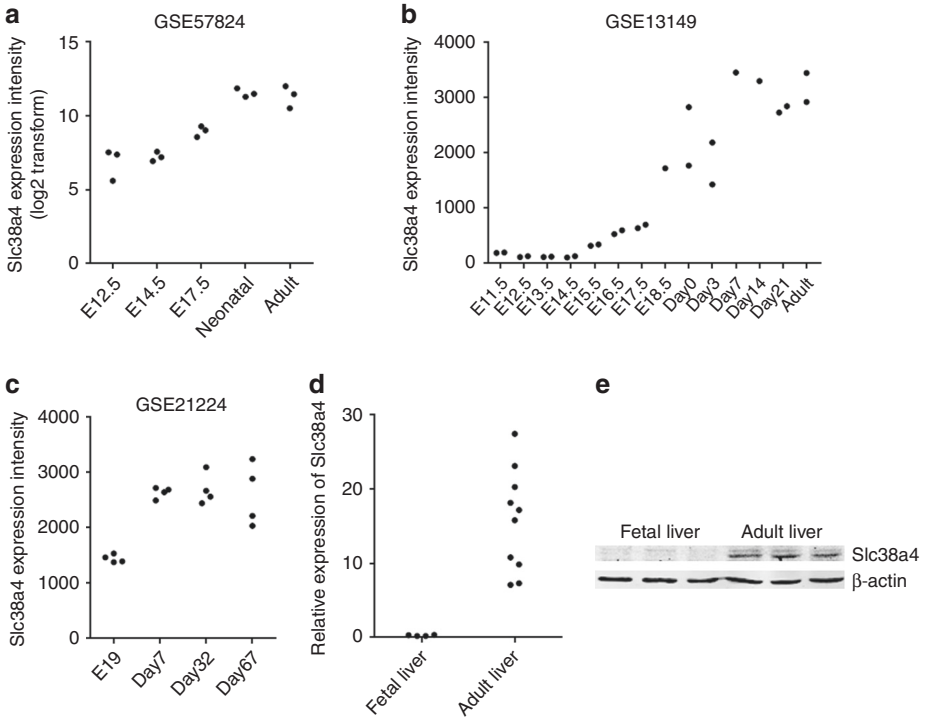

Fig. 1 Slc38a4 is downregulated in foetal livers compared with adult livers. a Slc38a4 expression levels during mouse liver development from the GSE57824 dataset. $P = 0.0003$ by Kruskal–Wallis test. **b** Slc38a4 expression levels during mouse liver development from the GSE13149 dataset. **c** Slc38a4 expression levels during mouse liver development from GSE21224 dataset. $P = 0.0208$ by Kruskal–Wallis test. **d** qRT-PCR analyses of Slc38a4 expression in mouse adult liver tissues ($n = 10$) and foetal liver tissues ($n = 4$). $P = 0.0020$ by Mann–Whitney test. **e** Western blot analyses of Slc38a4 expression in mouse foetal liver and adult liver tissues.

nontumor liver tissues (Fig. 2h). Collectively, these data demonstrated that SLC38A4 was downregulated in HCC, and low SLC38A4 expression was correlated with high serum AFP, poor differentiation, advanced clinical staging and poor prognosis of HCC patients.

DNA methylation contributes to the downregulation of SLC38A4

Epigenetic alterations are closely related to gene expressions [19, 20]. Intriguingly, we identified a CpG island CpG64 at the promoter of human *SLC38A4* (Fig. 3a). The CpG island CpG36 was also identified at the promoter of mouse *Slc38a4* (Fig. 3a). To determine whether DNA methylation regulates SLC38A4 expression, Huh7 and Hep3B cells were treated with the demethylation reagent 5-Aza. 5-Aza treatment significantly increased SLC38A4 mRNA and protein levels in both cells (Fig. 3b and Supplementary Fig. 2a). Furthermore, 5-Aza treatment reduced Huh7 xenograft growth in vivo and increased SLC38A4 expression in xenograft (Supplementary Fig. 2b, c). To determine whether the downregulation of Slc38a4 in mouse foetal liver is associated with DNA methylation alteration of CpG36, we measured the DNA methylation levels of CpG36 by bisulfate sequencing in three foetal liver tissues and three adult liver tissues. CpG36 DNA methylation levels were significantly higher in foetal liver tissues compared with those in adult liver tissues (Fig. 3c), supporting that CpG36 DNA hypermethylation contributed to Slc38a4 downregulation in the foetal liver. To determine whether DNA methylation contributes to SLC38A4 downregulation in human HCC tissues, four methylation probes located on CpG64 with available methylation data were retrieved from TCGA Illumina Infinium Human DNA Methylation 450k bead chip data to calculate the correlation between SLC38A4 expression and CpG64 methylation status. Pearson correlation analyses using TCGA LIHC samples having both methylation and SLC38A4 expression data revealed that all four probes in CpG64 were significantly inversely correlated with SLC38A4 expression (Fig. 3d). Furthermore, we measured the DNA methylation levels of CpG64 by bisulfate sequencing in five pairs of randomly selected human HCC tissues and adjacent nontumor liver tissues. CpG64 DNA methylation levels were significantly higher in HCC tissues compared with those in paired nontumor liver tissues (Fig. 3e), supporting that DNA methylation was involved in SLC38A4 downregulation in human HCC. CpG64 DNA methylation levels were higher in Hep3B cells compared with those in Huh7 cells (Supplementary Fig. 2d), which is consistent with the lower baseline expression of SLC38A4 in Hep3B cells than that in Huh7 cells (Fig. 3b). Collectively, these data suggested that DNA hypermethylation at least partially contributed to the downregulation of Slc38a4 in the foetal liver and the downregulation of SLC38A4 in HCC.

SLC38A4 depletion exerts oncogenic roles in HCC

Due to the significant correlation between low SLC38A4 expression and high serum AFP, poor differentiation, advanced clinical staging and poor prognosis, we next investigated the potential biological roles of SLC38A4 downregulation in HCC. Huh7 cells with SLC38A4 stable knockdown were constructed using SLC38A4-specific shRNA lentivirus (Fig. 4a). CCK-8 assays results showed that SLC38A4 depletion remarkably promoted Huh7 cellular proliferation (Fig. 4b). EdU incorporation assays also indicated that Huh7 cells with SLC38A4 stable knockdown had a significantly increased percentage of EdU-positive cells (Fig. 4c). In clone-formation assays, the number of clones formed by SLC38A4-depleted cells was much higher than that formed by control cells (Fig. 4d). Non-adherent spheroid culture assays revealed that SLC38A4 knockdown enhanced stemness-like activity of Huh7 cells (Fig. 4e). Annexin V staining and flow cytometry showed that SLC38A4 knockdown significantly repressed Huh7 cellular apoptosis (Fig. 4f). Transwell migration

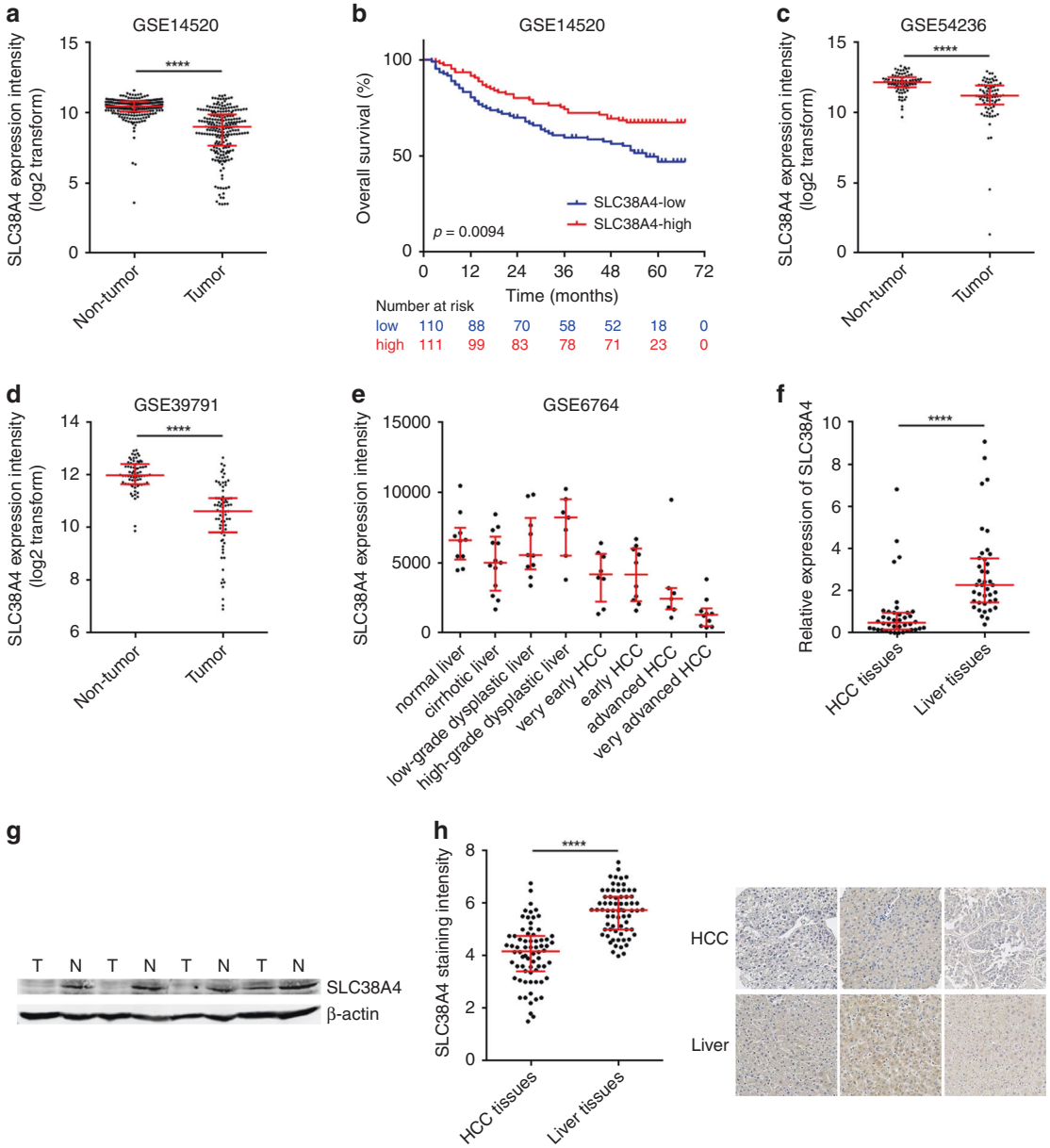

Fig. 2 SLC38A4 is downregulated in HCC tissues and negatively correlated with prognosis. a SLC38A4 expression intensity in HCC tissues ($n = 225$) and noncancerous liver tissues ($n = 220$) according to the GSE14520 dataset. **b** Kaplan–Meier survival analysis of the correlation between SLC38A4 expression and overall survival of HCC patients according to the GSE14520 dataset. $P = 0.0094$ by log-rank test. **c** SLC38A4 expression intensity in HCC tissues ($n = 81$) and noncancerous liver tissues ($n = 80$) according to the GSE54236 dataset. **d** SLC38A4 expression intensity in 72 pairs of HCC tissues and noncancerous liver tissues according to the GSE39791 dataset. **e** SLC38A4 expression intensity in human normal liver tissues ($n = 10$), cirrhotic liver tissues ($n = 13$), low-grade dysplastic liver tissues ($n = 10$), high-grade dysplastic liver tissues ($n = 7$), very early HCC tissues ($n = 8$), early HCC tissues ($n = 10$), advanced HCC tissues ($n = 7$) and very advanced HCC tissues ($n = 10$) according to GSE6764 dataset. $P < 0.0001$ by Kruskal–Wallis test. **f** qRT-PCR analysis of SLC38A4 expression in 40 pairs of HCC tissues and adjacent noncancerous liver tissues. **g** Western blot analysis of SLC38A4 expression in four pairs of human HCC tissues (T) and nontumor liver tissues (N). **h** IHC staining of SLC38A4 in human tissue array including 70 pairs of HCC tissues and nontumor liver tissues. For **a**, **c**–**f** and **h**, data are shown as median with interquartile range. ****$P < 0.0001$ by Mann–Whitney test (**a**, **c**) or Wilcoxon matched-pairs signed-rank test (**d**, **f**, **h**).

assays showed that SLC38A4 knockdown significantly promoted Huh7 cellular migration (Fig. 4g). Furthermore, Huh7 cells with SLC38A4 stable knockdown or control were subcutaneously injected into the armpit of athymic nude mice. Huh7 cells with SLC38A4 stable knockdown apparently formed much larger tumours than control Huh7 cells (Fig. 4h). To further confirm the effects of SLC38A4 depletion in HCC, we stably knocked down SLC38A4 using shRNA with a different target site (Supplementary Fig. 3a). CCK-8, EdU incorporation, clone formation, non-adherent spheroid culture, Annexin V staining and flow cytometry and transwell migration assays revealed that SLC38A4 depletion using another shRNA also promoted cellular proliferation, increased the number of clones formed, enhanced stemness-like activity, repressed cellular apoptosis and promoted cellular migration (Supplementary Fig. 3b–g). Collectively, these results demonstrated that SLC38A4 depletion promoted HCC cellular proliferation, stemness and migration, and inhibited HCC cellular apoptosis in vitro. SLC38A4 depletion also promoted HCC tumorigenesis in vivo, indicating that SLC38A4 depletion has oncogenic roles in HCC.

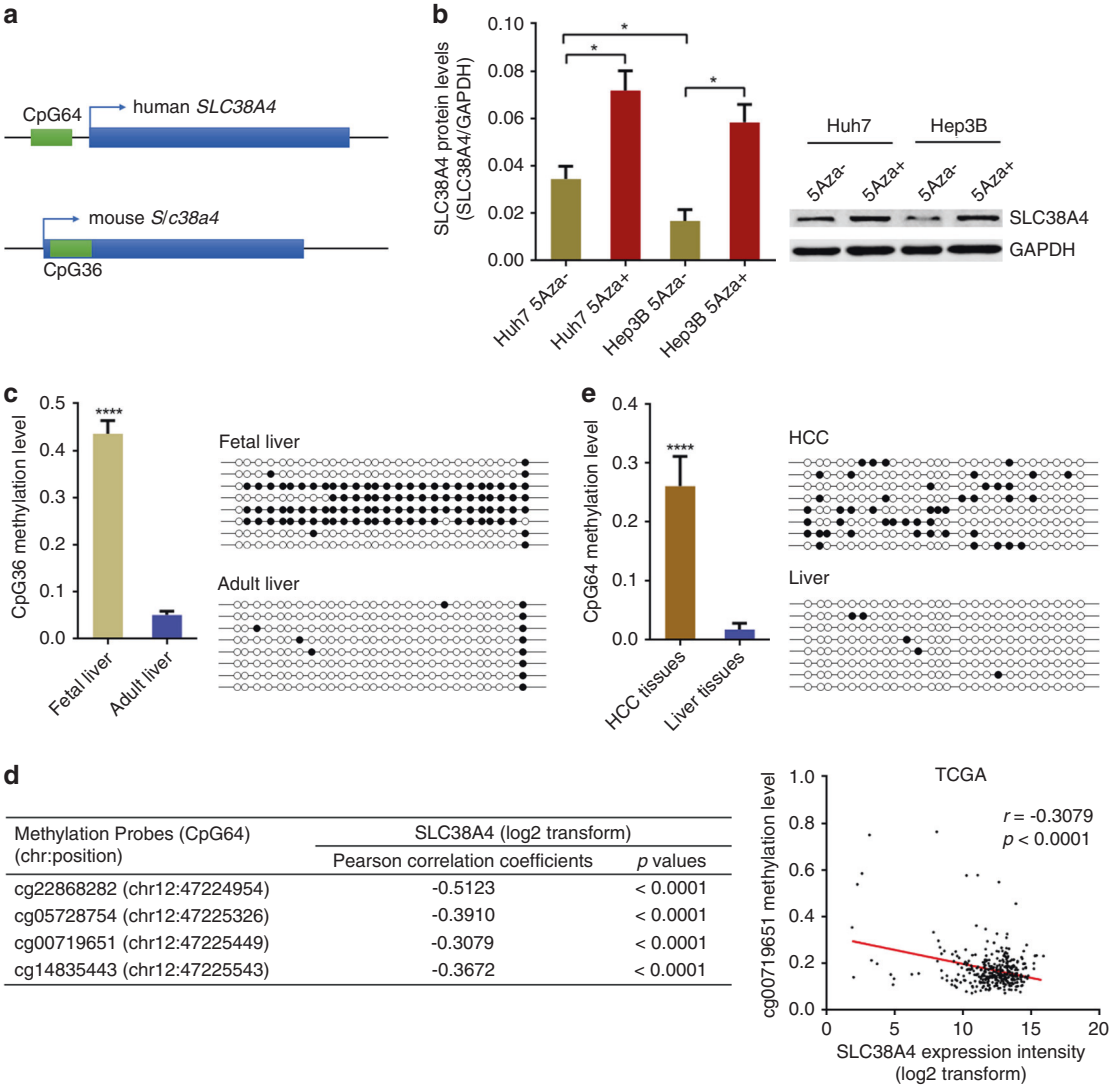

Methylation Probes (CpG64) (chr:position)	SLC38A4 (log2 transform)	
	Pearson correlation coefficients	*p* values
cg22868282 (chr12:47224954)	-0.5123	< 0.0001
cg05728754 (chr12:47225326)	-0.3910	< 0.0001
cg00719651 (chr12:47225449)	-0.3079	< 0.0001
cg14835443 (chr12:47225543)	-0.3672	< 0.0001

Fig. 3 DNA methylation contributes to the downregulation of SLC38A4. a Schematic structure of human *SLC38A4* and mouse *Slc38a4* genomic locus. Green boxes indicate the CpG islands. **b** Western blot analyses of SLC38A4 expression in Huh7 and Hep3B cells after treatment with 2.5 μM 5-Aza for 3 days. Data are shown as mean ± s.d. of $n = 3$ independent experiments. $^{*}P < 0.05$ by Student's *t* test. **c** Bisulfate DNA sequencing of CpG36 from three foetal liver tissues and three adult liver tissues. Data are shown as mean ± s.d. $^{****}P < 0.0001$ by Student's *t* test. **d** Correlation between SLC38A4 expression from TCGA LIHC dataset and methylation probes in CpG64 from TCGA Illumina Infinium Human DNA Methylation 450k bead chip in LIHC. Representative figure of correlation between SLC38A4 expression and methylation probe cg00719651 is shown on the right. **e** Bisulfate DNA sequencing of CpG64 from 5 pairs of human HCC tissues and nontumor liver tissues. Data are shown as mean ± s.d. $^{****}P < 0.0001$ by Student's *t* test.

SLC38A4 overexpression exerts tumour suppressive roles in HCC

To further confirm the biological roles of SLC38A4 in HCC, Hep3B cells with SLC38A4 stable overexpression were constructed using SLC38A4 overexpression lentivirus (Supplementary Fig. 4a). CCK-8 assays showed that SLC38A4 overexpression remarkably inhibited Hep3B cellular proliferation (Supplementary Fig. 4b). EdU incorporation assays further indicated that Hep3B cells with SLC38A4 overexpression had decreased percentage of EdU-positive cells (Supplementary Fig. 4c). In clone-formation assays, the number of clones formed by Hep3B cells with SLC38A4 overexpression was apparently lower than that formed by control cells (Supplementary Fig. 4d). Non-adherent spheroid culture assays revealed that SLC38A4 overexpression reduced stemness-like activity of Hep3B cells (Supplementary Fig. 4e). Annexin V staining and flow cytometry showed that SLC38A4 overexpression significantly promoted Hep3B cellular apoptosis (Supplementary Fig. 4f). Transwell migration assays showed that SLC38A4 overexpression significantly decreased Hep3B cellular migration (Supplementary Fig. 4g). Huh7 cells with SLC38A4 stable overexpression were also constructed using SLC38A4 overexpression vector (Supplementary Fig. 5a). CCK-8, EdU incorporation, clone formation, non-adherent spheroid culture, Annexin V staining and flow cytometry and transwell migration assays revealed that SLC38A4 overexpression in Huh7 cells also inhibited cellular proliferation, decreased the number of clones formed, reduced stemness-like activity, promoted cellular apoptosis and repressed cellular migration (Supplementary Fig. 5b–g). Collectively, these data demonstrated that SLC38A4 overexpression inhibited HCC cellular proliferation, stemness, and migration, and promoted HCC cellular apoptosis, indicating that SLC38A4 overexpression has tumour suppressive roles in HCC.

SLC38A4 upregulates HMGCS2 expression via repressing Wnt/β-catenin/MYC axis

Given that SLC38A4 is a neutral and cationic amino acids transporter, we detected amino acids concentrations in Huh7

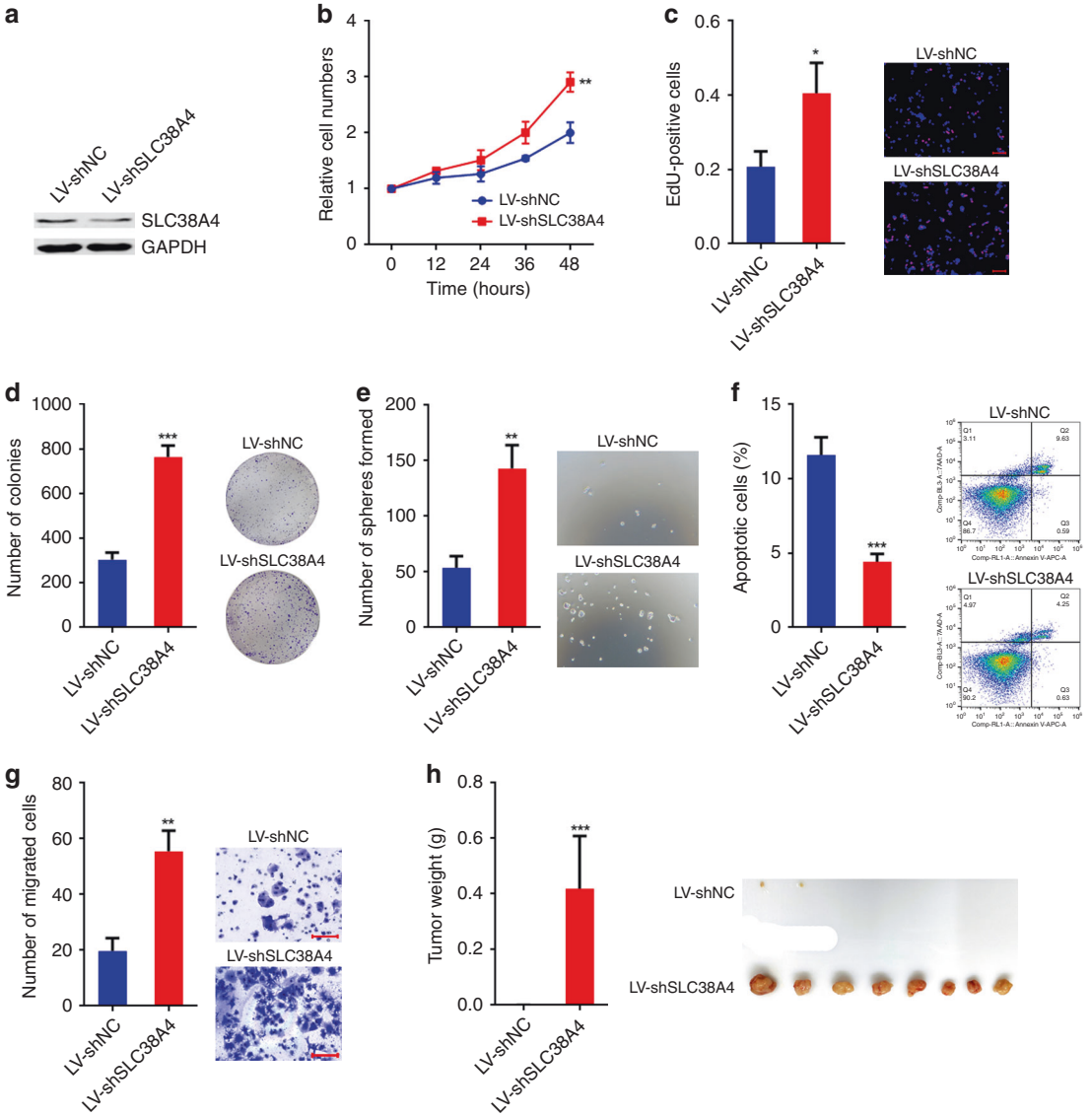

Fig. 4 SLC38A4 depletion exerts oncogenic roles in HCC. a Western blot analyses of SLC38A4 expression in Huh7 cells with SLC38A4 stable knockdown or control. **b** Cellular proliferation of Huh7 cells with SLC38A4 stable knockdown or control was measured using CCK-8 assays. **c** Cellular proliferation of Huh7 cells with SLC38A4 stable knockdown or control was assessed using EdU incorporation assays. Scale bar, 100 μm. **d** Colony formation assays of Huh7 cells with SLC38A4 stable knockdown or control. In total, 4000 cells were seeded and cultured for 10 days. **e** Non-adherent spheroid culture assays of Huh7 cells with SLC38A4 stable knockdown or control. **f** Cellular apoptosis of Huh7 cells with SLC38A4 stable knockdown or control after treatment with 2 μl/ml 3% H_2O_2 for 6 h was measured by Annexin V staining and flow cytometry. **g** Cellular migration of Huh7 cells with SLC38A4 stable knockdown or control was measured using transwell migration assays. Scale bar, 100 μm. **h** Weight and photo of subcutaneous tumours formed by Huh7 cells with SLC38A4 stable knockdown or control. Data are shown as mean ± s.d. of $n = 3$ independent experiments (**b**–**g**) or $n = 8$ mice in each group (**h**). *$P < 0.05$, **$P < 0.01$, ***$P < 0.001$ by Student's t test (**b**–**g**) or Mann–Whitney test (**h**).

cells after SLC38A4 depletion. As shown in Supplementary Fig. 6, the concentrations of alanine, histidine, glycine, valine and lysine were reduced in Huh7 cells after SLC38A4 depletion with fold changes of 0.565–0.835, which were consistent with the reported roles of SLC38A4 in amino acids uptake [15]. Amino acids are routinely required for tumour cells oncogenesis. Therefore, the oncogenic role of SLC38A4 depletion in HCC may be not dependent on the slight downregulations of amino acid concentrations.

To elucidate the underlying molecular mechanisms mediating the roles of SLC38A4 in HCC, we analysed TCGA LIHC dataset and the GSE14520 dataset to identify the genes whose expressions were positively or negatively correlated with SLC38A4 expression in HCC tissues. Four genes *ALDOB*, *HMGCS2*, *BHMT1* and *KNG1* with reported tumour suppressive roles were selected [21–24], whose expressions were positively correlated with SLC38A4 expression in both TCGA LIHC and GSE14520 datasets (Supplementary Table 3). Six genes *CLIC1*, *TCF3*, *FAM57A*, *MAPRE1*, *VOPP1* and *SMARCAL1* with reported oncogenic roles were selected [25–30], whose expressions were negatively correlated with SLC38A4 expression in both TCGA LIHC and GSE14520 datasets (Supplementary Table 3). The expressions of these ten candidate genes were measured in Hep3B cells with SLC38A4 overexpression and Huh7 cells with SLC38A4 knockdown (Fig. 5a, b). HMGCS2 (3-hydroxy-3-methylglutaryl CoA synthase 2) has the most significant upregulation after SLC38A4 overexpression and most significant

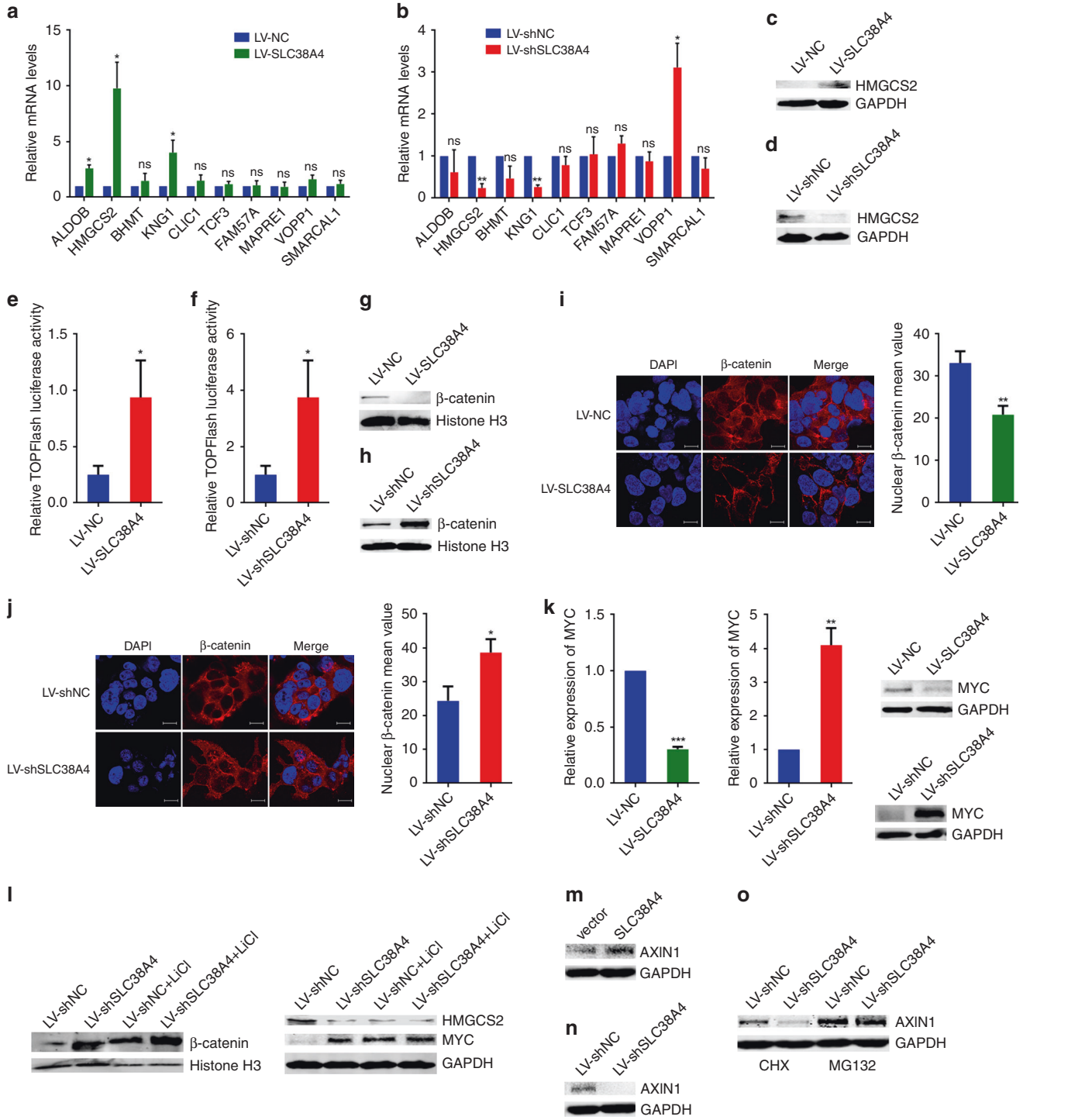

downregulation after SLC38A4 knockdown (Fig. 5a, b). The significantly positive correlation between SLC38A4 and HMGCS2 expression in HCC tissues was confirmed in TCGA LIHC, GSE54236, GSE14520 and GSE39791 datasets (Supplementary Fig. 7a–d). Consistent with HMGCS2 mRNA levels, HMGCS2 protein levels were also significantly upregulated after SLC38A4 overexpression and downregulated after SLC38A4 knockdown (Fig. 5c, d), indicating that SLC38A4 upregulated HMGCS2. HMGCS2 is a mitochondrial ketogenic enzyme, which was reported to be involved in intestinal cell differentiation, lipogenesis and various cancers [22, 31, 32]. Particularly, several reports revealed the tumour suppressive roles of HMGCS2 in HCC [22, 32, 33]. Thus, we further investigated the modulation of HMGCS2 by SLC38A4. MYC was previously reported to repress *HMGCS2* transcription [31]. Wnt/β-catenin signalling was revealed to decrease HMGCS2 protein and mRNA levels [34]. MYC is a well-known Wnt/β-catenin downstream target [35]. Wnt/β-catenin signalling is frequently reported to be involved in the development and HCC [10, 12]. Therefore, we further investigated the potential effects of SLC38A4 on the Wnt/β-catenin/MYC axis. The luciferase activity of β-catenin reporter TOPFlash was reduced after SLC38A4 overexpression and increased after SLC38A4 knockdown (Fig. 5e, f). Furthermore,

Fig. 5 SLC38A4 upregulates HMGCS2 expression via repressing Wnt/β-catenin/MYC. a qRT-PCR analyses of the expressions of ten candidate genes, whose expressions were positively or negatively correlated with SLC38A4 in HCC tissues, in Hep3B cells with SLC38A4 stable overexpression or control. **b** qRT-PCR analyses of the expressions of ten candidate genes, whose expressions were positively or negatively correlated with SLC38A4 in HCC tissues, in Huh7 cells with SLC38A4 stable knockdown or control. **c** Western blot analyses of HMGCS2 expressions in Hep3B cells with SLC38A4 stable overexpression or control. **d** Western blot analyses of HMGCS2 expressions in Huh7 cells with SLC38A4 stable knockdown or control. **e** β-catenin reporter TOPFlash was co-transfected with pRL-TK into Hep3B cells with SLC38A4 stable overexpression or control. Luciferase activities were measured 48 h after transfection. Results were presented as the relative ratio of firefly luciferase activity to Renilla luciferase activity. **f** β-catenin reporter TOPFlash was co-transfected with pRL-TK into Huh7 cells with SLC38A4 stable knockdown or control. Luciferase activities were measured 48 h after transfection. Results were presented as the relative ratio of firefly luciferase activity to Renilla luciferase activity. **g** Western blot analyses of nuclear β-catenin expression in Hep3B cells with SLC38A4 stable overexpression or control. **h** Western blot analyses of nuclear β-catenin expression in Huh7 cells with SLC38A4 stable knockdown or control. **i** Immunofluorescence staining of β-catenin in Hep3B cells with SLC38A4 stable overexpression or control showed reduced nuclear β-catenin after SLC38A4 overexpression. Scale bar, 15 μm. **j** Immunofluorescence staining of β-catenin in Huh7 cells with SLC38A4 stable knockdown or control showed increased nuclear β-catenin after SLC38A4 silencing. Scale bar, 15 μm. **k** qRT-PCR and western blot analyses of MYC expressions in Hep3B cells with SLC38A4 stable overexpression or control, and Huh7 cells with SLC38A4 stable knockdown or control. **l** Huh7 cells with SLC38A4 stable knockdown or control were treated with 20 mM LiCl for 24 h. Then, nuclear β-catenin expression and total HMGCS2 and MYC expression were detected by western blot. Histone H3 and GAPDH were used as a nuclear protein and total protein loading controls, respectively. **m** Western blot analyses of AXIN1 expressions in Huh7 cells with SLC38A4 stable overexpression or control. **n** Western blot analyses of AXIN1 expressions in Huh7 cells with SLC38A4 stable knockdown or control. **o** Huh7 cells with SLC38A4 stable knockdown or control were treated with 50 μg/ml CHX or 10 μM MG132 for 24 h, followed by detection of AXIN1 protein levels. Data are shown as mean ± s.d. of $n = 3$ independent experiments. $^{*}P < 0.05$, $^{**}P < 0.01$, $^{***}P < 0.001$, ns, not significant, by Student's *t* test.

western blot assays showed that nuclear β-catenin levels were reduced after SLC38A4 overexpression and increased after SLC38A4 knockdown (Fig. 5g, h and Supplementary Fig. 8a, b). IF assays also showed the reduced nuclear translocation of β-catenin after SLC38A4 overexpression and increased nuclear translocation of β-catenin after SLC38A4 knockdown (Fig. 5i, j). MYC mRNA and protein levels were both reduced after SLC38A4 overexpression and increased after SLC38A4 knockdown (Fig. 5k). These data suggested that SLC38A4 repressed Wnt/β-catenin signalling and downregulated MYC. To determine whether the regulation of HMGCS2 by SLC38A4 is dependent on Wnt/β-catenin signalling, Huh7 cells with SLC38A4 knockdown or control were treated with LiCl to activate Wnt/β-catenin signalling (Fig. 5l and Supplementary Fig. 8c). Similar to SLC38A4 knockdown, LiCl treatment activated Wnt/β-catenin signalling, upregulated MYC and repressed HMGCS2 expression (Fig. 5l). In the context of Wnt/β-catenin signalling activation, SLC38A4 knockdown did not further regulate MYC and HMGCS2 expression (Fig. 5l). Furthermore, we used β-catenin siRNA to repress Wnt/β-catenin signalling (Supplementary Fig. 8d). In the context of Wnt/β-catenin blocking, SLC38A4 knockdown did not further regulate MYC and HMGCS2 expression (Supplementary Fig. 8e). These data suggested that the regulation of HMGCS2 by SLC38A4 was dependent on Wnt/β-catenin signalling. To investigate the mechanism by which SLC38A4 represses Wnt/β-catenin signalling, we detected the potential effects of SLC38A4 on Wnt/β-catenin pathway components, including LRP6, DVL2, and β-catenin degradation complex. Intriguingly, AXIN1, the major component of β-catenin degradation complex, was remarkably upregulated after SLC38A4 overexpression and downregulated after SLC38A4 depletion (Fig. 5m, n). AXIN1 mRNA levels were not changed after SLC38A4 overexpression or depletion (Supplementary Fig. 8f, g). To investigate whether SLC38A4 regulates AXIN1 protein synthesis or degradation, SLC38A4-depleted Huh7 cells were treated with protein synthesis inhibitor cycloheximide (CHX) and proteasome inhibitor MG132. The change of AXIN1 protein level was largely abolished by MG132, but not by CHX (Fig. 5o), suggesting that SLC38A4 increased AXIN1 protein stability. Collectively, these data demonstrated that SLC38A4 upregulated HMGCS2 expression via upregulating AXIN1 and repressing Wnt/β-catenin/MYC axis.

The expression pattern of HMGCS2 is consistent with SLC38A4 during foetal liver development and HCC

To determine the expression pattern of Hmgcs2 during foetal liver development, GSE57824 and GSE13149 datasets were analysed. Consistent with Slc38a4, Hmgcs2 was gradually increased during the mouse liver development process (Fig. 6a, b). The expression of HMGCS2 in human HCC and its clinical relevance were further investigated. TCGA LIHC dataset showed that low HMGCS2 expression was remarkably correlated with poor overall survival, disease-specific survival, recurrence-free survival and progression-free survival (Supplementary Fig. 9a–d) analysed by Kaplan–Meier Plotter (https://kmplot.com/analysis/index.php). Correlation analyses between HMGCS2 expression levels and clinicopathological characteristics from TCGA LIHC dataset revealed that low HMGCS2 expression was significantly correlated with high serum AFP concentration, poor differentiation, advanced tumour pathologic pT staging and advanced TNM staging (Supplementary Table 4), indicating that consistent with SLC38A4, low HMGCS2 could also be regarded as an embryonic and potential oncogenic factor. GSE14520 dataset revealed that HMGCS2 was downregulated in HCC tissues compared with noncancerous liver tissues (Fig. 6c). Kaplan–Meier survival analysis consistently revealed that low HMGCS2 expression was significantly correlated with poor overall survival according to the GSE14520 dataset (Fig. 6d). Correlation analyses between HMGCS2 expression levels and clinicopathological characteristics from the GSE14520 dataset consistently revealed that low HMGCS2 expression was significantly correlated with high serum AFP concentration, high predicted risk metastasis signature, multinodular, liver cirrhosis, advanced TNM staging and advanced BCLC staging (Supplementary Table 5). The downregulation of HMGCS2 in HCC was further verified in GSE54236 and GSE39791 datasets (Fig. 6e, f). GSE6764 datasets revealed that the expression of HMGCS2 was gradually downregulated during the progression of HCC (Fig. 6g). HMGCS2 mRNA levels in the same 40 pairs of human HCC tissues and adjacent noncancerous liver tissues used in Fig. 2f were measured by qRT-PCR, and the results revealed that HMGCS2 mRNA levels were also downregulated in HCC tissues compared with liver tissues (Fig. 6h). A significantly positive correlation between SLC38A4 and HMGCS2 mRNA levels in these 40 HCC tissues was also observed (Supplementary Fig. 7e). IHC staining of HMGCS2 in the same human tissue array, including 70 pairs of HCC tissues and nontumor liver tissues used in Fig. 2h, also revealed significantly weaker staining density of HMGCS2 in HCC tissues compared with paired nontumor liver tissues (Fig. 6i and Supplementary Fig. 10). A significantly positive correlation between SLC38A4 and HMGCS2 IHC staining intensities was also observed in these 70 HCC tissues (Supplementary Fig. 7f). Collectively, these data demonstrated that consistent with SLC38A4, HMGCS2 was downregulated in HCC,

and low HMGCS2 expression was correlated with high serum AFP, poor differentiation, advanced clinical staging and poor prognosis of HCC patients. The expression pattern of HMGCS2 during foetal liver development and HCC further supported the regulation of HMGCS2 by SLC38A4 in vivo.

HMGCS2 reverses the roles of SLC38A4 silencing in HCC

HMGCS2 was reported to have tumour suppressive roles in HCC [22, 32]. Therefore, we further confirm whether HMGCS2 also has tumour repressive roles in our models. Huh7 cells with HMGCS2 stable overexpression were constructed via transfection of HMGCS2 overexpression vector (Supplementary Fig. 11a). CCK-8, EdU incorporation, clone formation, non-adherent spheroid culture, Annexin V staining and flow cytometry and transwell migration assays revealed that HMGCS2 overexpression inhibited cellular proliferation, decreased the number of clones formed, reduced stemness-like activity, promoted cellular apoptosis and repressed cellular migration (Supplementary Fig. 11b–g), confirming that HMGCS2 exerts tumour suppressive roles in HCC. To determine whether HMGCS2 is a downstream mediator of the oncogenic roles of SLC38A4 silencing in HCC, HMGCS2 was stably overexpressed in Huh7 cells with SLC38A4 stable knockdown via transfection of HMGCS2 overexpression vector (Supplementary Fig. 12a). CCK-8 assays results showed that HMGCS2 overexpression reversed the accelerated cell proliferation caused by SLC38A4 knockdown (Supplementary Fig. 12b). EdU incorporation assays also indicated that HMGCS2 overexpression reversed the increased percentage of EdU-positive cells caused by SLC38A4 knockdown (Supplementary Fig. 12c). In clone-formation assays, HMGCS2 overexpression reversed the increased number of clones caused by SLC38A4 knockdown (Supplementary Fig. 12d). Non-adherent spheroid culture assays revealed that HMGCS2 overexpression reversed the enhanced stemness-like activity of Huh7 cells caused by SLC38A4 knockdown (Supplementary Fig. 12e). Annexin V staining and flow cytometry showed that HMGCS2 overexpression reversed the reduced cell apoptosis caused by SLC38A4 knockdown (Supplementary Fig. 12f). Transwell migration assays showed that HMGCS2 overexpression reversed the increased cell migration caused by SLC38A4 knockdown (Supplementary Fig. 12g). Collectively, these results demonstrated that HMGCS2 overexpression reversed the oncogenic roles of SLC38A4 silencing in HCC.

DISCUSSION

Hepatocellular carcinoma is one of the deadliest malignancies [11, 36, 37]. Those HCCs with progenitor-like features are revealed to have worse outcome [8]. Identifying the shared oncofetal molecular events between foetal liver and HCC tissues would provide new avenues for recognising more malignant HCCs with worse prognoses. These oncofetal molecular events represent potential therapeutic targets for HCC.

In this study, we identified the unique expression pattern of SLC38A4-silenced in foetal liver, activated in adult liver and re-silenced in HCC tissues. Thus, SLC38A4 silencing was regarded as an oncofetal molecular event in HCC. SLC38A4 silencing was indeed correlated with a worse prognosis of HCC, supported by several cohorts. The correlation between low SLC38A4 expression and high serum AFP concentration, poor differentiation of HCC tissues supported SLC38A4 silencing as an oncofetal molecular event. Therefore, these findings proposed that SLC38A4 is a potential prognostic biomarker for HCC. The prognostic value of SLC38A4 could be further verified by prospective studies. AFP is a well-known HCC diagnostic biomarker. The correlation between low SLC38A4 expression and high serum AFP concentration suggested that SLC38A4 concentration in peripheral blood may be a potential diagnostic marker for HCC, which needs further investigation.

SLC38A4 is a membrane protein that is predominantly expressed in the liver (GTEx RNA-Seq data). As an imprinted gene, *Slc38a4* is maternally DNA methylated and predominantly paternally expressed in the foetus [38]. *Slc38a4* is reported to be repressed by DNA methylation and H19-MBD1 complex-mediated H3K9me3 in mouse embryo fibroblasts [39]. EHMT2 is reported to maintain germline-derived DNA methylation at *Slc38a4* gene imprinted locus in embryos [40]. In this study, we further confirmed that DNA methylation repressed SLC38A4 expression. Methylation levels of *Slc38a4* in foetal liver tissues were remarkably higher than those in adult liver tissues. In human HCC tissues, we also found a significant inverse correlation between *SLC38A4* DNA methylation level and SLC38A4 expression level. Combining these previous reports, our novel findings further supported that DNA methylation contributes to the silence of SLC38A4/Slc38a4 in foetal liver, activation in adult liver, and re-silence in HCC tissues.

Except for the dysregulated expression and prognostic value of SLC38A4 in HCC, we also documented that SLC38A4 has tumour suppressive roles in HCC. Our results showed that SLC38A4 knockdown promoted HCC cellular proliferation, stemness, migration, and inhibited HCC cellular apoptosis in vitro. SLC38A4 knockdown also promoted HCC tumorigenesis in vivo. SLC38A4 overexpression inhibited HCC cellular proliferation, stemness, migration, and promoted HCC cellular apoptosis. Overexpression or re-activation of SLC38A4, such as the removal of DNA methylation at the *SLC38A4* locus, represent new strategies for HCC treatment.

Amino acids are obligatory for the survival and growth of highly proliferative cells, such as embryonic cells and cancer cells [17]. Therefore, amino acid transporters are routinely highly expressed in these proliferative cells [18]. SLC1A5/ASCT2, another neutral amino acid transporter, is indispensable for leukaemia initiation and maintenance [41]. Tumour cells with high levels of methionine transporter SLC43A2 outcompeted T cells for methionine, which lead to loss of H3K79me2 in T cells and impairment of T-cell immunity [42]. In contrast to the reported oncogenic roles of amino acid transporters, here we identified SLC38A4 as a tumour suppressor in HCC. Therefore, we speculated that other mechanisms might mediate the tumour suppressive roles of SLC38A4 in HCC. Using co-expression analyses and experimental investigations, we identified HMGCS2 as a critical downstream target and functional mediator of SLC38A4 in HCC. SLC38A4 increased HMGCS2 expression via repressing Wnt/β-catenin/MYC axis. Further, we identified AXIN1 as the critical mediator between SLC38A4 and Wnt/β-catenin/MYC axis. SLC38A4 upregulated AXIN1 and therefore repressing Wnt/β-catenin signalling. The expression patterns of HMGCS2 during foetal liver development and in HCC are very similar to those of SLC38A4. Furthermore, the clinical relevance of HMGCS2 is also very similar to SLC38A4 in HCC, such as the association with AFP, differentiation, clinical staging, and prognosis. HMGCS2 is reported to induce ketone body production, induce mitochondrial fatty acid oxidation, and inhibit glycolysis via various mechanisms [22, 32, 34, 43–45]. Thus, we proposed that the SLC38A4/HMGCS2 regulatory axis may exert special influences on metabolism in HCC cells and represent novel connections between carbohydrate, amino acid, and fatty acid metabolism, which need further investigations.

In summary, we identified SLC38A4 silencing as an oncofetal molecular event in foetal liver development and HCC. SLC38A4/Slc38a4 is silenced in the foetal liver, activated in the adult liver and re-silenced in HCC. Low expression of SLC38A4 is associated with poor differentiation, advanced clinical staging, and worse prognosis in HCC. SLC38A4 exerts tumour suppressive roles in HCC via upregulating HMGCS2. SLC38A4 increases HMGCS2 expression via repressing Wnt/β-catenin/MYC axis. Similar to SLC38A4, HMGCS2/Hmgcs2 is also silenced in the foetal liver, activated in the adult liver and re-silenced in HCC. Low HMGCS2 expression is also associated with poor differentiation, advanced

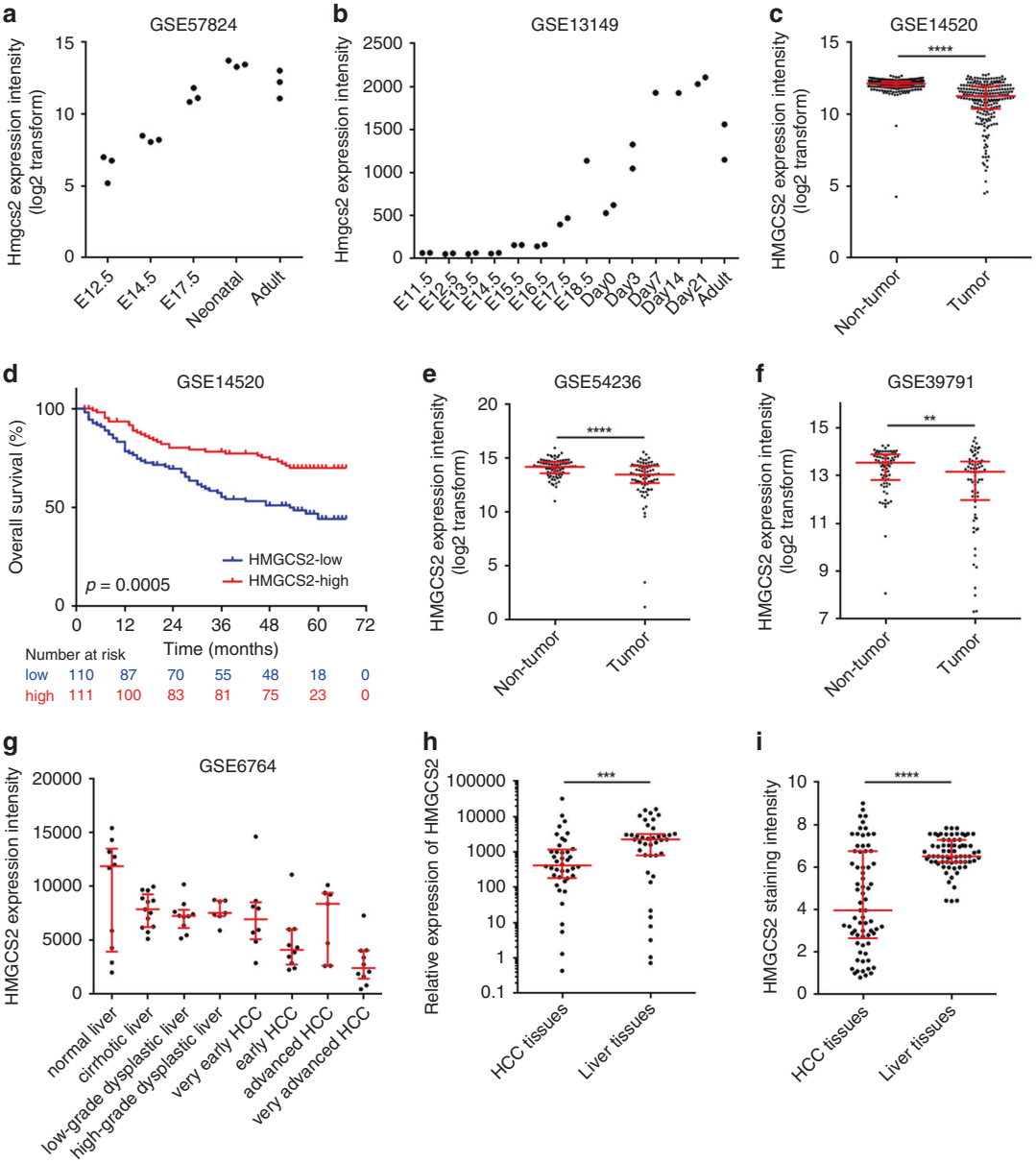

Fig. 6 The expression pattern of Hmgcs2/HMGCS2 during foetal liver development and HCC, and its clinical relevance in HCC. a Hmgcs2 expression levels during mouse liver development from GSE57824 dataset. $P < 0.0001$ by Kruskal–Wallis test. **b** Hmgcs2 expression levels during mouse liver development from GSE13149 dataset. **c** HMGCS2 expression intensity in HCC tissues ($n = 225$) and noncancerous liver tissues ($n = 220$) according to the GSE14520 dataset. **d** Kaplan–Meier survival analysis of the correlation between HMGCS2 expression and overall survival of HCC patients according to GSE14520 dataset. $P = 0.0005$ by log-rank test. **e** HMGCS2 expression intensity in HCC tissues ($n = 81$) and noncancerous liver tissues ($n = 80$) according to the GSE54236 dataset. **f** HMGCS2 expression intensity in 72 pairs of HCC tissues and noncancerous liver tissues according to the GSE39791 dataset. **g** HMGCS2 expression intensity in human normal liver tissues ($n = 10$), cirrhotic liver tissues ($n = 13$), low-grade dysplastic liver tissues ($n = 10$), high-grade dysplastic liver tissues ($n = 7$), very early HCC tissues ($n = 8$), early HCC tissues ($n = 10$), advanced HCC tissues ($n = 7$) and very advanced HCC tissues ($n = 10$) according to GSE6764 dataset. $P = 0.0005$ by Kruskal–Wallis test. **h** qRT-PCR analysis of HMGCS2 expression in 40 pairs of HCC tissues and adjacent noncancerous liver tissues. **i** IHC staining of HMGCS2 in human tissue array including 70 pairs of HCC tissues and nontumor liver tissues. For **c** and **e**–**i**, data are shown as median with interquartile range. $^{**}P < 0.01$, $^{***}P < 0.001$, $^{****}P < 0.0001$ by Mann–Whitney test (**c**, **e**) or Wilcoxon matched-pair signed-rank test (**f**, **h**, **i**).

clinical staging, and worse prognosis in HCC. Thus, SLC38A4/HMGCS2 regulatory axis represent oncofetal molecular events, prognostic biomarkers and therapeutic targets for HCC.

DATA AVAILABILITY

The bioinformatic data were deposited in the Cancer Genome Atlas (TCGA)-Liver Hepatocellular Carcinoma (LIHC) and Gene Expression Omnibus (GEO) database (https://www.ncbi.nlm.nih.gov/geo/) with accession numbers GSE57824, GSE13149, GSE21224, GSE14520, GSE54236, GSE39791 and GSE6764. The other data generated or analysed are included in this article or available from the corresponding author upon reasonable request.

REFERENCES

1. Bray F, Ferlay J, Soerjomataram I, Siegel RL, Torre LA, Jemal A. Global cancer statistics 2018: GLOBOCAN estimates of incidence and mortality worldwide for 36 cancers in 185 countries. CA: A Cancer J Clin. 2018;68:394–424.

2. Siegel RL, Miller KD, Fuchs HE, Jemal A. Cancer statistics, 2021. CA: A Cancer J Clin. 2021;71:7–33.
3. Ahronian LG, Zhu LJ, Chen YW, Chu HC, Klimstra DS, Lewis BC. A novel KLF6-Rho GTPase axis regulates hepatocellular carcinoma cell migration and dissemination. Oncogene. 2016;35:4653–62.
4. Xue R, Chen L, Zhang C, Fujita M, Li R, Yan SM, et al. Genomic and transcriptomic profiling of combined hepatocellular and intrahepatic cholangiocarcinoma reveals distinct molecular subtypes. Cancer cell. 2019;35:932–47 e938.
5. Hernanda PY, Chen K, Das AM, Sideras K, Wang W, Li J, et al. SMAD4 exerts a tumor-promoting role in hepatocellular carcinoma. Oncogene. 2015;34:5055–68.
6. Ahodantin J, Bou-Nader M, Cordier C, Megret J, Soussan P, Desdouets C, et al. Hepatitis B virus X protein promotes DNA damage propagation through disruption of liver polyploidization and enhances hepatocellular carcinoma initiation. Oncogene. 2019;38:2645–57.
7. Urtasun R, Elizalde M, Azkona M, Latasa MU, Garcia-Irigoyen O, Uriarte I, et al. Splicing regulator SLU7 preserves survival of hepatocellular carcinoma cells and other solid tumors via oncogenic miR-17-92 cluster expression. Oncogene. 2016;35:4719–29.
8. Becker D, Sfakianakis I, Krupp M, Staib F, Gerhold-Ay A, Victor A, et al. Genetic signatures shared in embryonic liver development and liver cancer define prognostically relevant subgroups in HCC. Mol Cancer. 2012;11:55.
9. Lee JS, Heo J, Libbrecht L, Chu IS, Kaposi-Novak P, Calvisi DF, et al. A novel prognostic subtype of human hepatocellular carcinoma derived from hepatic progenitor cells. Nat Med. 2006;12:410–6.
10. Llovet JM, Kelley RK, Villanueva A, Singal AG, Pikarsky E, Roayaie S, et al. Hepatocellular carcinoma. Nat Rev Dis Prim. 2021;7:6.
11. Kudo Y, Sugimoto M, Arias E, Kasashima H, Cordes T, Linares JF, et al. PKClambda/iota loss induces autophagy, oxidative phosphorylation, and NRF2 to promote liver cancer progression. Cancer Cell. 2020;38:247–262 e211.
12. Yamashita T, Wang XW. Cancer stem cells in the development of liver cancer. J Clin Investig. 2013;123:1911–8.
13. Wang F, Yuan JH, Wang SB, Yang F, Yuan SX, Ye C, et al. Oncofetal long noncoding RNA PVT1 promotes proliferation and stem cell-like property of hepatocellular carcinoma cells by stabilizing NOP2. Hepatology. 2014;60:1278–90.
14. Shi Q, Padmanabhan R, Villegas CJ, Gu S, Jiang JX. Membrane topological structure of neutral system N/A amino acid transporter 4 (SNAT4) protein. J Biol Chem. 2011;286:38086–94.
15. Matoba S, Nakamuta S, Miura K, Hirose M, Shiura H, Kohda T, et al. Paternal knockout of Slc38a4/SNAT4 causes placental hypoplasia associated with intrauterine growth restriction in mice. Proc Natl Acad Sci USA. 2019;116:21047–53.
16. Kondou H, Kawai M, Tachikawa K, Kimoto A, Yamagata M, Koinuma T, et al. Sodium-coupled neutral amino acid transporter 4 functions as a regulator of protein synthesis during liver development. Hepatol. Res. 2013;43:1211–23.
17. Broer S. The SLC38 family of sodium-amino acid co-transporters. Pflug Arch: Eur J Physiol. 2014;466:155–72.
18. Pizzagalli MD, Bensimon A, Superti-Furga G. A guide to plasma membrane solute carrier proteins. FEBS J. 2021;288:2784–835.
19. Nguyen DH, Soygur B, Peng SP, Malki S, Hu G, Laird DJ. Apoptosis in the fetal testis eliminates developmentally defective germ cell clones. Nat Cell Biol. 2020;22:1423–35.
20. Carrot-Zhang J, Chambwe N, Damrauer JS, Knijnenburg TA, Robertson AG, Yau C, et al. Comprehensive analysis of genetic ancestry and its molecular correlates in cancer. Cancer Cell. 2020;37:639–654 e636.
21. Tao QF, Yuan SX, Yang F, Yang S, Yang Y, Yuan JH, et al. Aldolase B inhibits metastasis through Ten-Eleven Translocation 1 and serves as a prognostic biomarker in hepatocellular carcinoma. Mol Cancer. 2015;14:170.
22. Wang YH, Liu CL, Chiu WC, Twu YC, Liao YJ. HMGCS2 mediates ketone production and regulates the proliferation and metastasis of hepatocellular carcinoma. Cancers. 2019;11:1876.
23. Teng YW, Mehedint MG, Garrow TA, Zeisel SH. Deletion of betaine-homocysteine S-methyltransferase in mice perturbs choline and 1-carbon metabolism, resulting in fatty liver and hepatocellular carcinomas. J Biol Chem. 2011;286:36258–67.
24. Xu J, Fang J, Cheng Z, Fan L, Hu W, Zhou F, et al. Overexpression of the Kininogen-1 inhibits proliferation and induces apoptosis of glioma cells. J Exp Clin Cancer Res. CR. 2018;37:180.
25. Setti M, Savalli N, Osti D, Richichi C, Angelini M, Brescia P, et al. Functional role of CLIC1 ion channel in glioblastoma-derived stem/progenitor cells. J Natl Cancer Inst. 2013;105:1644–55.
26. Taniue K, Kurimoto A, Takeda Y, Nagashima T, Okada-Hatakeyama M, Katou Y, et al. ASBEL-TCF3 complex is required for the tumorigenicity of colorectal cancer cells. Proc Natl Acad Sci USA. 2016;113:12739–44.
27. Baltaci E, Seyhan B, Baykara O, Buyru N. CT120: a new potential target for c-Myc in head and neck cancers. J Cancer. 2017;8:880–6.
28. Kim K, Lee HC, Park JL, Kim M, Kim SY, Noh SM, et al. Epigenetic regulation of microRNA-10b and targeting of oncogenic MAPRE1 in gastric cancer. Epigenetics. 2011;6:740–51.
29. Bonin F, Taouis K, Azorin P, Petitalot A, Tariq Z, Nola S, et al. VOPP1 promotes breast tumorigenesis by interacting with the tumor suppressor WWOX. BMC Biol. 2018;16:109.
30. Zhang L, Fan S, Liu H, Huang C. Targeting SMARCAL1 as a novel strategy for cancer therapy. Biochem Biophys Res. Commun. 2012;427:232–5.
31. Camarero N, Mascaro C, Mayordomo C, Vilardell F, Haro D, Marrero PF. Ketogenic HMGCS2 is a c-Myc target gene expressed in differentiated cells of human colonic epithelium and down-regulated in colon cancer. Mol Cancer Res. MCR. 2006;4:645–53.
32. Wang YH, Suk FM, Liao YJ. Loss of HMGCS2 enhances lipogenesis and attenuates the protective effect of the ketogenic diet in liver cancer. Cancers. 2020;12:1797.
33. Su SG, Yang M, Zhang MF, Peng QZ, Li MY, Liu LP, et al. miR-107-mediated decrease of HMGCS2 indicates poor outcomes and promotes cell migration in hepatocellular carcinoma. Int J Biochem Cell Biol. 2017;91:53–9.
34. Kim JT, Li C, Weiss HL, Zhou Y, Liu C, Wang Q, et al. Regulation of ketogenic enzyme HMGCS2 by Wnt/beta-catenin/PPARgamma pathway in intestinal cells. Cells. 2019;8:1106.
35. Trautmann M, Sievers E, Aretz S, Kindler D, Michels S, Friedrichs N, et al. SS18-SSX fusion protein-induced Wnt/beta-catenin signaling is a therapeutic target in synovial sarcoma. Oncogene. 2014;33:5006–16.
36. Ma L, Hernandez MO, Zhao Y, Mehta M, Tran B, Kelly M, et al. Tumor cell biodiversity drives microenvironmental reprogramming in liver cancer. Cancer Cell. 2019;36:418–430 e416.
37. Hermanns C, Hampl V, Holzer K, Aigner A, Penkava J, Frank N, et al. The novel MKL target gene myoferlin modulates expansion and senescence of hepatocellular carcinoma. Oncogene. 2017;36:3464–76.
38. Smith RJ, Dean W, Konfortova G, Kelsey G. Identification of novel imprinted genes in a genome-wide screen for maternal methylation. Genome Res. 2003;13:558–69.
39. Monnier P, Martinet C, Pontis J, Stancheva I, Ait-Si-Ali S, Dandolo L. H19 lncRNA controls gene expression of the Imprinted Gene Network by recruiting MBD1. Proc Natl Acad Sci USA. 2013;110:20693–8.
40. Auclair G, Borgel J, Sanz LA, Vallet J, Guibert S, Dumas M, et al. EHMT2 directs DNA methylation for efficient gene silencing in mouse embryos. Genome Res. 2016;26:192–202.
41. Ni F, Yu WM, Li Z, Graham DK, Jin L, Kang S, et al. Critical role of ASCT2-mediated amino acid metabolism in promoting leukaemia development and progression. Nat Metab. 2019;1:390–403.
42. Bian Y, Li W, Kremer DM, Sajjakulnukit P, Li S, Crespo J, et al. Cancer SLC43A2 alters T cell methionine metabolism and histone methylation. Nature. 2020;585:277–82.
43. Vila-Brau A, De Sousa-Coelho AL, Mayordomo C, Haro D, Marrero PF. Human HMGCS2 regulates mitochondrial fatty acid oxidation and FGF21 expression in HepG2 cell line. J Biol Chem. 2011;286:20423–30.
44. Shimazu T, Hirschey MD, Hua L, Dittenhafer-Reed KE, Schwer B, Lombard DB, et al. SIRT3 deacetylates mitochondrial 3-hydroxy-3-methylglutaryl CoA synthase 2 and regulates ketone body production. Cell Metab. 2010;12:654–61.
45. Wang Q, Zhou Y, Rychahou P, Fan TW, Lane AN, Weiss HL, et al. Ketogenesis contributes to intestinal cell differentiation. Cell Death Differ. 2017;24:458–68.

ACKNOWLEDGEMENTS

We thank the Core Facility of Basic Medical Sciences, Shanghai Jiao Tong University School of Medicine for technical assistance.

AUTHOR CONTRIBUTIONS

J-HY designed the study. J-HY, FW and S-HS supervised the study. JL, M-HL, T-TW, X-NL, X-TZ, K-CZ, Y-DL, Y-ZD and J-LL performed the experiments. J-HY and R-LG evaluated the IHC data. J-HY and T-TW wrote the paper. The data and the manuscript have been discussed and approved by all authors.

FUNDING INFORMATION

This work was supported by grants from the Shanghai Rising-Star Program (18QA1405100), the National Natural Science Foundation of China (Grant Nos. 81830085, 92059111, 81972738, 81773005 and 81672775), and the National Key Basic Research Program (973 projects) (2015CB554004) from the Ministry of Science and Technology of China.

ETHICS APPROVAL AND CONSENT TO PARTICIPATE

This study was performed with the approval of the Committee on Ethics of Biomedicine Research, Naval Medical University.

CONSENT TO PUBLISH

All authors consent to this manuscript to be published.

COMPETING INTERESTS

The authors declare no competing interests.

ADDITIONAL INFORMATION

Supplementary information The online version contains supplementary material available at https://doi.org/10.1038/s41416-021-01490-y.

Correspondence and requests for materials should be addressed to F.W. or J.-h.Y.

Reprints and permission information is available at http://www.nature.com/reprints

Publisher's note Springer Nature remains neutral with regard to jurisdictional claims in published maps and institutional affiliations.